LLR- based Bit- loading Algorithm and its Applications to HomePlug AV over OPERA Power- line Channels with Impulsive Noise

Eleonora Guerrini[1], Lorenzo Guerrieri[1], Daniele Veronesi[2], Paola Bisaglia[1], Roberto Cappelletti[3]
[1]Dora S.p.A, STMicroelectronics Group, Via Lavoratori Vittime del Col du Mont 28, 11100 Aosta, Italy
[2]MGTech s.r.l., Via Verdi, 14, 24100 Bergamo, Italy
[3]STMicroelectronics s.r.l., Via Tolomeo 1, 20010 Cornaredo (MI), Italy
Email: eleonora-dora-spa.guerrini@st.com

Abstract— **In this paper the higher data rate technology of HomePlug, called HomePlug AV, is tested over the power-line channel models proposed by the OPERA project coupled with the Middleton Class A impulsive noise model. In particular the DLC bit-loading algorithm is developed and the performance is analyzed in terms of throughput when different scenarios are considered. To better exploit the error correction capabilities of the turbo code, this bit-loading algorithm attempts to maximize the throughput while guaranteeing a target BER over a set of sub-carriers using a new metric based on the LLRs. Simulations show that the effect of the impulsive noise can be reduced by inserting a clipping module before the OFDM demodulator, thus guaranteeing very promising throughputs even in the worst scenarios.**

Index Terms— **Bit-loading, HomePlug AV, OFDM, power-line channel.**

I. Introduction

HOMEPLUG is an alliance of more than 75 companies formed in 2000 to define specifications for power-line communication systems. In July 2005, HomePlug released HomePlug AV (HPAV) [1], [2], the latest generation technology for the in-home distribution of audio and video data, aimed at satisfying very high data rates and quality of service requirements. HPAV supports raw data rates up to 150 Mbit/s, employing adaptive orthogonal frequency division multiplexing (OFDM) over a bandwidth from 1.8 to 30 MHz. The possible modulations that may be employed per OFDM sub-carrier are: BPSK, QPSK, 8-QAM, 16-QAM, 64-QAM, 256-QAM and 1024-QAM. Robust performance is reached through the use of a turbo convolutional code [3] and a proper bit-loading algorithm, which, however, is not specified in [1].

A suitable bit-loading algorithm for HPAV should maximize the overall throughput while guaranteeing a target bit error rate (BER) with uniform power allocation. An example of a frequently adopted algorithm with a very low complexity is the *BER threshold constant* (BTC) [4]. In this paper an iterative discrete rate-adaptive algorithm with uniform power allocation, referred as *decreasing LLR-constrained* (DLC) algorithm [4], is presented. In order to better exploit the error correction capabilities of the turbo code, this algorithm shifts the target BER into a constraint on a new metric, which is based on the log-likelihood ratios (LLRs) fed into the decoder. In this analysis some results of [4] are revisited and the theory of the DLC is enlarged. Another major intent is to investigate on the performance of the HPAV system further, with the DLC bit-loading algorithm, under different realistic power-line environments affected by impulsive noise [5].

In the literature, the power-line channel is studied using two different approaches: i) frequency-domain (multi-conductor transmission line), where the description of the network properties is based on the physical network characteristics (cable geometry, losses, etc.) [6], [7]; ii) time-domain (multi-path), where a phenomenological or statistical description is given, based on on-field measurements [8], [9], [10]. In this analysis the time-domain approach is preferred since it is more general and it does not require a perfect knowledge of all the properties of the line. In order to simulate different working conditions, characterized by several multi-path realizations and background noise, the channel models proposed by the open power-line communication European research alliance (OPERA) project [10], [11] are here considered. To the authors knowledge the herein results are the first showing the HPAV technology with the OPERA deliverables. As already noted by Babic et al. [12], in the field of broadband power-line communications, "the most important developments are certainly being carried out by the OPERA and HomePlug Alliances". Furthermore, impulsive noise, which is the most critical aspect in power-line transmissions [13] is added to the OPERA channel models and several scenarios, characterized by different degrees of impulsiveness, are presented. Clipping [14], in the form of amplitude nulling, is also considered to mitigate the effect of the impulsive noise. In order to include the effect of the channel and signal-to-noise ratio

This paper is based on "HomePlug AV system and DLC bit-loading algorithm over OPERA power-line channels with impulsive noise," by E. Guerrini, L. Guerrieri and D. Veronesi which appeared in the Proceedings of the 12th IEEE Int. Symposium on Power Line Communications and Its Applications (ISPLC), Jeju Island, Korea, April 2008. Manuscript received Oct.1, 2008; accepted Nov. 19, 2008.

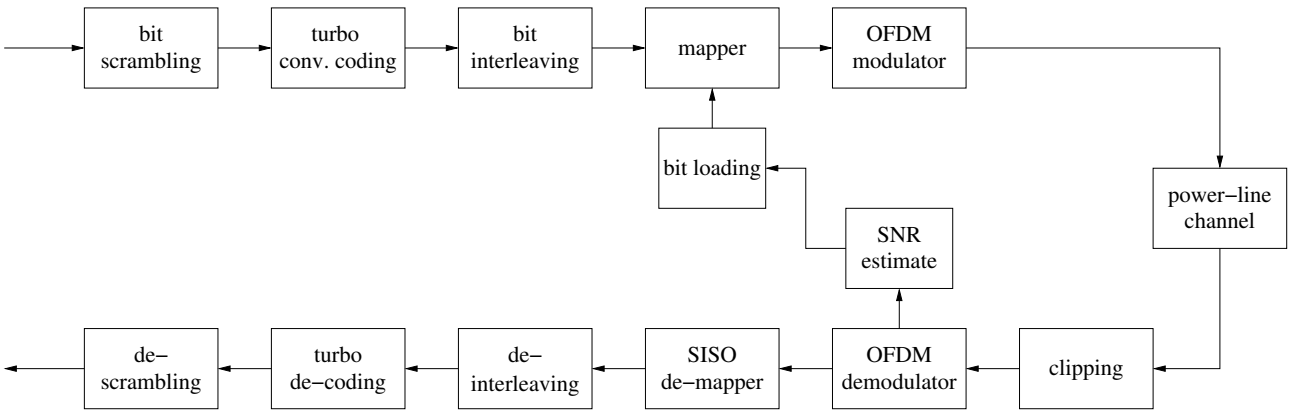

Figure 1. Block diagram of the HPAV physical layer for data transmission.

(SNR) estimates on the system's performance, results with data-aided estimators are also reported. The remainder of this paper is organized as follows: in Section II the physical layer of the HPAV system is reviewed and in Section III the bit-loading algorithm is presented. In Section IV the channel model is described, showing the different scenarios where the performance of the HPAV system is analyzed. In Section V the adopted clipping technique is detailed. Numerical results are reported in Section VI, with conclusions given in Section VII. Finally, some technical details relating to the proposed bit-loading algorithm are shown in the Appendix.

II. System model

In Fig. 1 the considered HPAV physical layer [1], [2] is shown[1]. At the transmitter, the information bits are scrambled and fed into a turbo convolutional encoder with code rate R. The coded sequences are then bit-by-bit interleaved and converted into symbols, belonging to one of the available constellations, through a bit-mapper. Successively, the data symbols are serial-to-parallel converted for OFDM modulation. In HPAV the OFDM modulation is implemented by using a 3072-point inverse discrete Fourier transform (IDFT); however, to comply with frequency regulatory bodies, only 917 sub-carriers are employed for useful transmission. In order to remove both inter-symbol and inter-carrier interference (ISI and ICI), a suitable cyclic prefix is used.

At the receiver, after a clipping block, the cyclic prefix is removed and the OFDM demodulation is implemented by using a 3072-point discrete Fourier transform (DFT). Through this work the following assumptions are made: the cyclic prefix completely eliminates ISI and ICI; perfect synchronization is guaranteed; and the channel is time invariant within several OFDM symbols. The received signal, during the generic OFDM symbol over the sub-carrier k, for $k = 1, \ldots, N$, where N is the number of allocable sub-carriers, can be written as:

$$y_k = \sqrt{E_s} G_k a_k + n_k \ , \tag{1}$$

where E_s, a_k, G_k and n_k denote the transmitted symbol energy, the transmitted symbol, the channel frequency response complex coefficient and the complex additive noise with variance σ_k^2, over the k-th sub-carrier, respectively.

The output from the OFDM demodulator is then sent to a soft-input soft-output (SISO) de-mapper, a de-interleaver and a turbo convolutional decoder, which, in our solution, implements the Bahl, Cocke, Jelinek and Raviv (BCJR) algorithm [15] in an improved Max-Log-MAP form [16]. Successively, the bits provided by the decoder are de-scrambled in order to obtain an estimate of the transmitted bits.

Channel and SNR estimations are critical and essential elements in every turbo decoder and bit-loading algorithm. We employ data-aided per sub-carrier channel and SNR estimators, using known QPSK symbols transmitted during special packets, referred to as packets sound[2] [1]. Both the algorithms are described in [4], where a least square (LS) channel and a modified squared signal-to-noise variance (SNV) estimators are used to compute the channel frequency response and the SNR value, respectively.

In the following section, details on how the SISO de-mapper has been implemented are given in order to introduce various parameters used in Section III.

A. SISO de-mapper

Let $\mathcal{H}$ be one of the possible HPAV constellations, with m bits per symbol (i.e.[3] $m = \log_2 |\mathcal{H}|$). The complex symbol transmitted over the sub-carrier k is denoted with a_k, while the corresponding coded bits sequence is denoted with $\{c_{1,k}, \ldots, c_{m,k}\}$. For each bit $c_{i,k}$, with $i = 1, \ldots, m$, the constellation $\mathcal{H}$ is split into two partitions of complex symbols associated to the coded bits sequence with a '0' in position i, namely $S_i^{(0)}$, and the

[1] As explained in [2], the bits are differently structured by the HPAV transmitter depending on whether they are data or control information. In this paper, for the sake of simplicity, we will refer to the HPAV data format.

[2] The packets sound are available in the HPAV system before starting the useful data transmission.

[3] $|\mathcal{H}|$ denotes the number of elements in $\mathcal{H}$.

complementary partition, $S_i^{(1)}$. Let $z_k = y_k/(\sqrt{E_s}G_k)$ be the equalized signal. Introducing the notation

$$D_{i,k} = \frac{1}{4}\left(\min_{\alpha\in S_i^{(0)}} |z_k-\alpha|^2 - \min_{\alpha\in S_i^{(1)}} |z_k-\alpha|^2\right) \quad (2)$$

the LLR of the bit $c_{i,k}$, with $i = 1, \ldots, m$, provided by the SISO de-mapper, can be approximated by [3]

$$\ell_{i,k} = \ln\left(\frac{P[c_{i,k}=1|y_k]}{P[c_{i,k}=0|y_k]}\right) \approx \underbrace{\frac{E_s|G_k|^2}{\sigma_k^2}}_{\gamma_k}\cdot 2\cdot D_{i,k}\ , \quad (3)$$

where $E_s|G_k|^2/\sigma_k^2 = \gamma_k$ is the SNR over the sub-carrier k. Approximated expressions of $\{D_{i,k}\}$ can be found in [3].

III. Bit-loading algorithms

In the following sections the BTC algorithm is revisited; furthermore, the DLC bit-loading algorithm is described.

A. BER threshold constant (BTC) algorithm

The BTC algorithm attempts to maximize the overall throughput of the system with a uniform power allocation, guaranteeing a target BER per sub-carrier [4]. For the coded HPAV system, the BER performance as a function of the SNR can be obtained by simulations [3]. Consequently, for each constellation an equivalent SNR constraint can be fixed for a given target BER. Let $\gamma^{(m_k,T)}$ denote the SNR constraint when m_k bits are loaded on the k-th sub-carrier, and let $\mathcal{C} = \{1, 2, 3, 4, 6, 8, 10\}$ be the set of all the possible numbers of bits that can be mapped into the generic symbol a_k. The problem solved by the BTC is:

$$\begin{cases} \max\limits_{m_k\in\mathcal{C}} \ m_k \\ \text{s.t. } \gamma_k \geq \gamma^{(m_k,T)} \end{cases} \qquad k = 1, \ldots, N\ . \quad (4)$$

The algorithm employs a memory look-up table, which contains the equivalent SNR constraint value, for each allowable modulation.

B. Decreasing LLR-constrained (DLC) algorithm

To better exploit the error correction capabilities of the turbo code, the key ideas of the DLC algorithm are: i) shifting the target BER, $P_e^{(T)}$, into an LLRs constraint, and ii) guaranteeing the target BER over a set of sub-carriers, whose indices belong to $\mathcal{T} \subseteq \{i : 1 \leq i \leq N\}$, instead of over a single sub-carrier (as done in the BTC). Some new useful definitions are introduced in Sections III-B.1 and III-B.2, before detailing the steps of the algorithm in Section III-B.3.

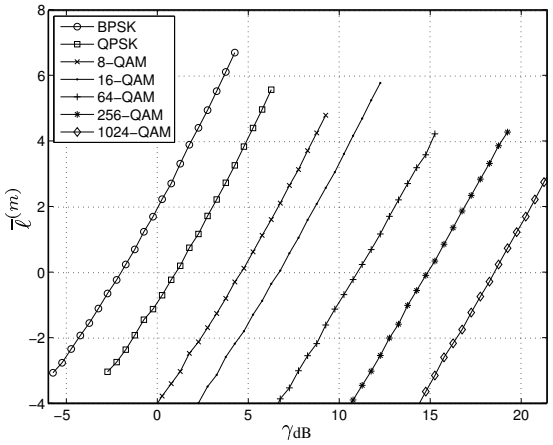

Figure 2. Metric given in (5) versus γ_{dB}, for all the HPAV allowable constellations.

1) Metric of LLRs: Let us first consider a single-carrier coded system, over an additive white Gaussian noise (AWGN) channel, with an SNR γ. We assume that the transmitted symbols belong to a constellation $\mathcal{H}$, with $\log_2(|\mathcal{H}|) = m$. Furthermore, let ℓ_i, with $i = 1, 2, \ldots, m$, be the LLR for the i-th bit that a SISO de-mapper provides to a soft-input decoder. In this framework, the introduced metric is the following[4]

$$\begin{aligned} \overline{\ell}^{(m)} &= \frac{1}{m}\sum_{i=1}^{m} \mathrm{E}\left[10\cdot\log_{10}|\ell_i|\right] \\ &= \gamma_{\text{dB}} + \underbrace{\frac{1}{m}\sum_{i=1}^{m}\mathrm{E}\left[10\cdot\log_{10}|2\cdot D_i|\right]}_{\Delta^{(m)}}\ . \end{aligned} \quad (5)$$

where $\gamma_{\text{dB}} = 10\log_{10}\gamma$. Although $\Delta^{(m)}$ depends on γ, from simulation results we can assert that $\Delta^{(m)}$ can be approximated to a constant value, in the range of interest. This is shown in Fig. 2, where the metric (5) is depicted versus γ_{dB}, for all the HPAV allowable constellations. As a consequence of (5), the target BER, that in the BTC algorithm was shifted into an SNR constraint (as in (4)), can here be shifted into an LLRs constraint as follows:

$$\overline{\ell}^{(m)} \geq \overline{\ell}^{(m,T)}\ , \quad (6)$$

where $\overline{\ell}^{(m,T)} = \gamma_{\text{dB}}^{(m,T)} + \Delta^{(m)}$. In an adaptive multi-carrier system, such as the considered HPAV, each sub-carrier can be loaded with a different constellation. Therefore, an extension of the metric in (5), that weighs the contribution given by each sub-carrier of the set $\mathcal{T}$ by taking into account the loaded modulation, is:

$$\overline{\ell} = \sum_{k\in\mathcal{T}} m_k\cdot\overline{\ell}_k^{(m_k)} \Big/ \sum_{k\in\mathcal{T}} m_k\ , \quad (7)$$

where $\overline{\ell}_k^{(m_k)}$ is the metric in (5), detailed to the k-th sub-carrier. Similarly to (6), the LLRs constraint for the HPAV

[4] $E[a]$ denotes the expectation of the random variable a.

system is

$$\overline{\ell} \geq \overline{\ell}^{(T)} \ , \tag{8}$$

where $\overline{\ell}^{(T)}$, hereafter referred to as the target LLR, can be obtained with different methods as reported in the Appendix.

2) Updating of the metric: Let $\mathcal{M} \subseteq \mathcal{T}$ be the set of sub-carrier indices where a bit-allocation of m'_k bits, with $k \in \mathcal{M}$, is chosen instead of the bit-allocation of m_k bits. The metric in (7), generated by a bit allocation m'_k, with $k \in \mathcal{M}$, and by m_k, with $k \in \{i : i \in \mathcal{T}, i \notin \mathcal{M}\}$, can be expressed as:

$$\overline{\ell}' = \frac{\sum\limits_{k\in\mathcal{T}} m_k \overline{\ell}_k^{(m_k)} - \sum\limits_{k\in\mathcal{M}} m_k \overline{\ell}_k^{(m_k)} + \sum\limits_{k\in\mathcal{M}} m'_k \overline{\ell}_k^{(m'_k)}}{\sum\limits_{k\in\mathcal{T}} m_k - \sum\limits_{k\in\mathcal{M}} m_k + \sum\limits_{k\in\mathcal{M}} m'_k} \tag{9}$$

Defining the cost of shifting from the bit-allocation m_k to the bit-allocation m'_k, on sub-carrier $k \in \mathcal{M}$, as

$$w_k = m'_k \overline{\ell}_k^{(m'_k)} - m_k \overline{\ell}_k^{(m_k)} \ , \tag{10}$$

the relationship between the metric $\overline{\ell}'$ and the metric $\overline{\ell}$, of (7), becomes:

$$\overline{\ell}' = \frac{\overline{\ell} \sum\limits_{k\in\mathcal{T}} m_k + \sum\limits_{k\in\mathcal{M}} w_k}{\sum\limits_{k\in\mathcal{T}} m_k + \sum\limits_{k\in\mathcal{M}} (m'_k - m_k)} \ . \tag{11}$$

3) Problem formulation: The proposed bit-loading algorithm attempts to maximize the system throughput with a uniform power allocation, while guaranteeing an LLRs constraint (equivalently to a target BER) over the set of sub-carriers $\mathcal{T}$. Consequently, the new problem can be summarized as[5]:

$$\begin{cases} \max\limits_{\{m_k\}\in\mathcal{C}^{|\mathcal{T}|}} \sum\limits_{k\in\mathcal{T}} m_k \\ \text{s.t. } \overline{\ell} \geq \overline{\ell}^{(T)} \end{cases} \ . \tag{12}$$

4) Problem solution: In short, the new algorithm starts with the bit allocation $\{m_k\}$, with $k \in \mathcal{T}$, provided by the BTC, as given in Section III-A. Since the BTC solution in general satisfies the constraint in (12) with a large margin, this algorithm can shift some sub-carriers in $\mathcal{T}$ from one constellation to the immediately higher constellation. In the explanation that follows the steps of the above algorithm are detailed:

1) Evaluate a first bit-allocation $\{m_k\}$, with $k \in \mathcal{T}$, based on the BTC algorithm;
2) Determine the bit-allocation $\{m'_k\}$, with $k \in \mathcal{T}$, that corresponds to the immediately higher bit-allocation;
3) Calculate by (10) the cost w_k, $\forall\, k \in \mathcal{T}$;
4) Search for the indices $\{\chi_1, \chi_2, \ldots, \chi_{|\mathcal{T}|}\}$, such that: $w_{\chi_1} > w_{\chi_2} > \ldots > w_{\chi_{|\mathcal{T}|}}$;
5) With a dichotomy search algorithm [17], determine the sub-carriers that can be loaded with a higher constellation, such that the constraint in (12) is still satisfied. The steps of the search algorithm are:
   a) Initialize ξ and its limits: $\xi = \lceil |\mathcal{T}|/2 \rceil$, LOW = 0, and UP = $|\mathcal{T}|$;
   b) Define the sub-set $\mathcal{M} = \{\chi_i : 1 \leq i \leq \xi\}$;
   c) Determine $\overline{\ell}'$ by (11);
   d) If $\overline{\ell}' \geq \overline{\ell}^{(T)}$, then update the lower limits and ξ: LOW $\leftarrow \xi$ and $\xi \leftarrow \lceil$(LOW + UP)$/2 \rceil$;
   e) If $\overline{\ell}' < \overline{\ell}^{(T)}$, then update the upper limits and ξ: UP $\leftarrow \xi$ and $\xi \leftarrow \lfloor$(LOW + UP)$/2 \rfloor$;
   f) If ($\xi \neq$ LOW & $\xi \neq$ UP) $\|$ $\overline{\ell}' < \overline{\ell}^{(T)}$, then goto b);
   g) Return $\mathcal{M}$.
6) Load m'_k bits on sub-carrier $k \in \mathcal{M}$ and m_k bits on sub-carrier $k \in \{i : i \in \mathcal{T}, i \notin \mathcal{M}\}$;
7) STOP.

Hereafter, this bit-loading algorithm will be referred as *decreasing LLR-constrained (DLC) algorithm.*

C. Comparison between the BTC and the DLC algorithms

In order to compare the BTC and the DLC algorithms, a multi-path channel[6] with AWGN noise is considered. Here and in the following sections, the HPAV cyclic prefix of 576 samples and the code rate $R = 1/2$ are adopted. With these assumptions the maximum achievable raw data rate is 95 Mbit/s. The target BER is fixed to 10^{-3} for both the algorithms. Performance is given in terms of average system throughput versus average received SNR. In this section, channel and SNR knowledge is assumed at the receiver. The throughput is calculated by averaging the loaded bits over many channel realizations. Fig. 3 shows that the DLC algorithm outperforms the BTC at every SNR value. For example, at an SNR $= 5$ dB and 15 dB, gains in throughput of 6.8 Mbit/s and 9.13 Mbit/s, respectively, are observed. In the next sections the performance of the DLC algorithm will be investigated with more realistic noise models.

IV. Channel Model

To model in-house networks, the channel and background noise models recently proposed by OPERA are used [10]. An indoor power-line essentially comprises the wiring and the electrical devices connected to it. The wiring can be modeled as a set of interconnected transmission lines terminated in loads that characterize the devices behavior. The loads show different impedances, highly varying with frequency. For this reason there are many impedance discontinuities producing reflections and echoes of the transmission signal. Hence, the power-line channel can be regarded as a multi-path environment where each transmitted signal reaches the receiver not only on a direct path, but also on delayed, and in most

[5] $\mathcal{C}^N$ denotes the set $\underbrace{\mathcal{C} \times \mathcal{C} \times \cdots \times \mathcal{C}}_{N \text{ times}}$.

[6] The multi-path channel is the OPERA "good" model described in Section IV.

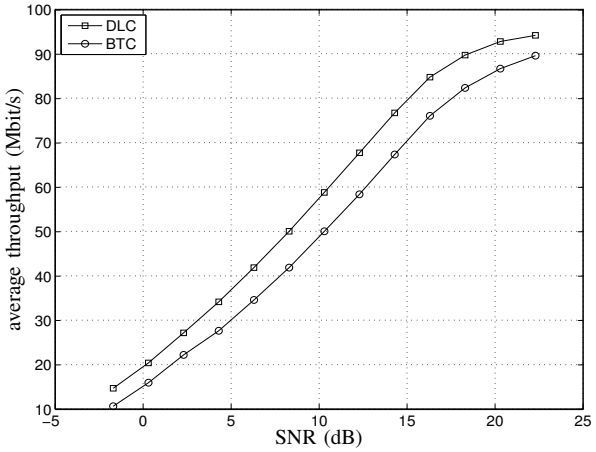

Figure 3. Performance of BTC and DLC algorithms: average HPAV throughput versus average received SNR in a multi-path channel with AWGN noise.

cases, attenuated paths. OPERA proposes four different reference models, hereafter classified as "good", "fair", "poor" and "bad" depending on their different selectivity and attenuation. For each model the number of paths P, the impulse response duration $T_{\rm h}$, the initial delay of the first path t_0, the range $[\Phi_{\rm min}, \Phi_{\rm max}]$ of the path amplitudes, and the root-mean-square delay spread $\tau_{\rm rms}$ are detailed in Tab. I.

Starting from these default values, different impulse response realizations can randomly be generated. A detailed description is given in [10].

As regards noise in power-line, two kinds of noise are considered, namely background noise and impulsive noise. The colored background noise is mainly caused by a superposition of numerous noise sources of low intensity. Its power spectral density (PSD) decreases with increasing frequency and it can be considered stationary since it varies over time in terms of minutes and hours. Results of multiple measurements of noise showed that the PSD can be approximated by an exponential decaying curve in logarithmic scale, as described in [10]:

$$B(f) = B_\infty + B_0 \cdot e^{-f/f_0} \ , \qquad (13)$$

where B_∞ is the PSD for $f \to \infty$, while B_0 is the difference between the maximum value of the PSD and B_∞. The third parameter f_0 represents the decaying exponential rate. In our analysis, $B_\infty = -136$ dB (V^2/Hz), $B_0 = -38$ dB (V^2/Hz) and $f_0 = 0.7$ MHz. The impulsive

TABLE I.
SET OF PARAMETERS OF THE MULTI-PATH MODEL PROPOSED BY OPERA.

Model	P	$T_{\rm h}[\mu$s]	$t_0[\mu$s]	$\Phi_{\rm min}$	$\Phi_{\rm max}$	$\tau_{\rm rms}[\mu$s]
good	5	0.5	0.2	0.005	0.05	0.096
fair	10	1.0	0.2	0.002	0.01	0.243
poor	15	1.5	0.5	0.0003	0.003	0.294
bad	20	2.0	0.5	0.0001	0.0005	0.474

noise, due to multiple sources such as power supplies or commutation of switches, is considered the main cause of burst error occurrence because of its high amplitudes and its strong time variance. The Middleton's Class A noise model [18] is considered a suitable statistical model to represent the impulsive noise in power-line channels [19], [20]. According to the model the samples of the noise are computed as a combination of background Gaussian noise and impulsive noise. In particular, let X be a random variable characterizing the Middleton's Class A noise, its probability density function (PDF) is given by

$$p_X(x) = \sum_{n=0}^{\infty} \frac{1}{\sqrt{2\pi\sigma_n^2}} \alpha_n \exp\left(-\frac{|x|^2}{2\sigma_n^2} \right) , \qquad (14)$$

where $\alpha_n = e^{-A}\frac{A^n}{n!}$, $\sigma_n^2 = \frac{n/A+\Gamma}{1+\Gamma}\sigma^2$, with σ^2 denoting the Class A noise variance, and $\Gamma = \sigma_g^2/\sigma_i^2$, where σ_g^2 is the background Gaussian variance and σ_i^2 is the impulsive noise variance ($\sigma^2 = \sigma_i^2 + \sigma_g^2$). A denotes the index of the impulsive noise. For small values of A the noise is highly impulsive, while when $A \to \infty$ the Class A noise approaches Gaussian characteristics. The Class A noise samples, which are characterized by the PDF in (14), can be obtained via the following equation:

$$\eta = x_{\rm G} + \sqrt{K_n} y \ , \qquad (15)$$

where $x_{\rm G}$ represents a white Gaussian background noise with zero-mean and variance σ_g^2, K_n is a statistically independent Poisson random variable, having mean A, and y is another white Gaussian sequence with zero-mean and variance σ_i^2/A. In our simulations, $x_{\rm G}$ is set to zero and the samples of noise are generated by

$$\eta = x_{\rm B} + \sqrt{K_n} y \ , \qquad (16)$$

where $x_{\rm B}$ are the samples of the colored background noise with PSD given by (13).

A. Description of the analyzed scenarios

The intent of this section is to describe the working conditions we considered during our simulations, referred as *scenarios*. A scenario is defined by: i) the channel frequency response, and ii) the Middleton's Class A parameters.

Among the power-line channel models proposed by OPERA first the "good" channel was chosen. Moreover, in order to investigate the system performance in more critical conditions, the "poor" channel was used, where the frequency selectivity and the signal attenuation increase. As regards the impulsive noise, the basic Middleton's Class A parameters here employed are:

- A: is the "impulsive index" [18], [21]. It is the product of the mean number of pulses per second and the mean length of a pulse in seconds. Small A means a low number of pulse events, but with high amplitude. As A is enlarged, the number of pulse events increases, but the probability of high amplitude pulses decreases, and when $A \to \infty$ the overall noise approaches the colored background noise.

Thus, A is a measure of the "impulsiveness" of the noise. A quasi-Gaussian environment is simulated with $A = 10$. In order to increase the impulsiveness of the noise $A = 10^{-1}$ (low impulsive) and 10^{-2} (impulsive) are considered. Finally, a very impulsive scenario is obtained with $A = 10^{-3}$.

- σ_i^2: is the mean power of the impulsive component of the noise. In our simulations σ_i^2 varies in the range $[10^{-8}, 10^{-2}]$.

In Tab. II the parameters of each scenario are detailed.

V. Mitigation of impulsive noise

A simple method of reducing the detrimental effect of the impulsive noise is the insertion of a clipping block before the OFDM demodulator, as shown in Fig. 1. Basic principles of clipping are studied in [14], where a method based on the following non-linear function was considered:

$$r_{\text{clipped}}(t) = \begin{cases} 0, & |r(t)| > \beta_{\text{clip}} \\ r(t), & |r(t)| \leq \beta_{\text{clip}} \end{cases}, \qquad (17)$$

$r(t)$ being the received signal in the time-domain and β_{clip} the clipping level. As explained in [14] this method, referred as amplitude nulling, is the best choice when the impulses are correctly detected. On the other hand, a distortion on the signal is always introduced, therefore the clipping value β_{clip} must be properly selected. In our simulations it is fixed to 2.8 times the mean peak of the absolute value of the received signal $r(t)$.

VI. Numerical Results

In this section the performance of the HPAV system, using the DLC bit-loading algorithm, is investigated in terms of average system throughput versus the average received SNR. In order to test how the system deals with various realistic environments the performance is compared over the different scenarios defined in Section IV-A. The throughput is calculated by averaging the allocated bits of the bit-loading algorithm over many realizations of the considered scenario. In the following results the number of OFDM symbols used to estimate the channel and the SNR per sub-carrier within the packets sound is fixed to 40, while the target BER is fixed to 10^{-3}. To satisfy this target, as explained in [4], a margin on the target LLR is introduced to cope with the channel and SNR estimate errors. Furthermore, compared to [4], since the DLC metrics are tailored to an AWGN system, the margin must also take into account the presence of the impulsive noise. Hereafter, for the sake of simplicity, we will refer to scenarios $\mathcal{S}_1$, $\mathcal{S}_2$, $\mathcal{S}_3$, and $\mathcal{S}_4$ as "good" scenarios, and to scenarios $\mathcal{S}_5$, $\mathcal{S}_6$, $\mathcal{S}_7$, and $\mathcal{S}_8$ as "poor" scenarios.

TABLE II.
SCENARIO PARAMETERS.

Scenario	OPERA Model	A
$\mathcal{S}_1$ *(good, quasi-Gaussian)*	good	10
$\mathcal{S}_2$ *(good, low impulsive)*	good	10^{-1}
$\mathcal{S}_3$ *(good, impulsive)*	good	10^{-2}
$\mathcal{S}_4$ *(good, very impulsive)*	good	10^{-3}
$\mathcal{S}_5$ *(poor, quasi-Gaussian)*	poor	10
$\mathcal{S}_6$ *(poor, low impulsive)*	poor	10^{-1}
$\mathcal{S}_7$ *(poor, impulsive)*	poor	10^{-2}
$\mathcal{S}_8$ *(poor, very impulsive)*	poor	10^{-3}

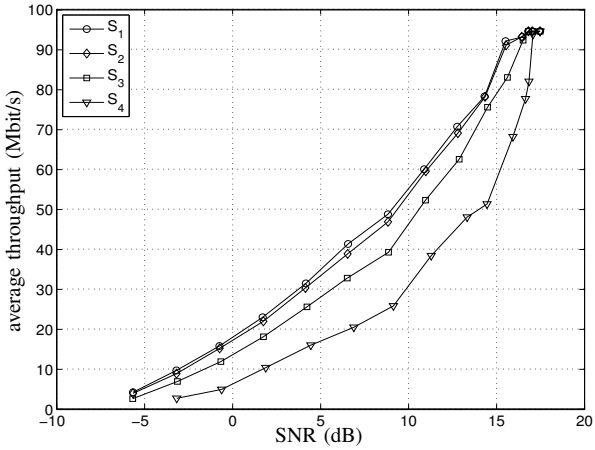

Figure 4. Average HPAV throughput versus average received SNR in "good" scenarios with noise "quasi-Gaussian" (S_1), "low impulsive" (S_2), "impulsive" (S_3) and "very impulsive" (S_4). The clipping block is not included.

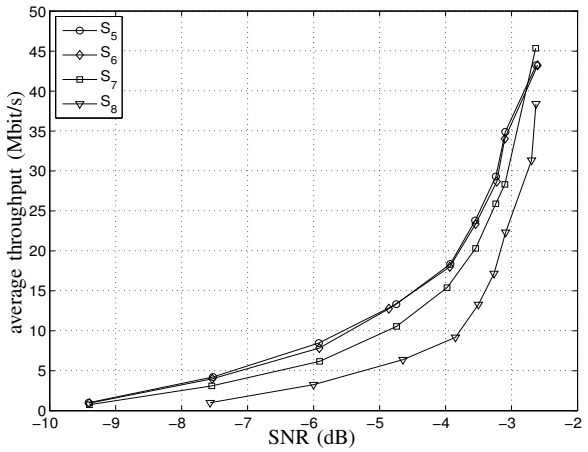

Figure 5. Average HPAV throughput versus average received SNR in "poor" scenarios with noise "quasi-Gaussian" (S_5), "low impulsive" (S_6), "impulsive" (S_7) and "very impulsive" (S_8). The clipping block is not included.

First, in Fig. 4 and Fig. 5, results without the insertion of the clipping block are shown. In Fig. 4, results are depicted for the "good" scenarios. We note that all these scenarios, at the higher SNRs, allow to reach the HPAV maximum achievable throughput of nearly 95 Mbit/s. As was expected, the best system performance is obtained in the "quasi-Gaussian" environment $\mathcal{S}_1$, while a degradation is observed as the scenario impulsiveness increases. In fact, the throughput reduction is negligible

in the "low impulsive" scenario with a loss of only 2.5% at an SNR $= 10$ dB. A more significant degradation is observed for the $\mathcal{S}_3$ and $\mathcal{S}_4$ environments: at an SNR $= 10$ dB the throughput reduction in the "impulsive" and "very impulsive" scenarios is 16% and 44%, respectively. A similar trend can be observed in Fig. 5 for the "poor" scenarios. For instance, let us consider an average received SNR of -4 dB. In the "low impulsive" environment the observed throughput reduction is only 1% compared to the "quasi-Gaussian" case. The losses are more consistent in the S_7 and S_8 environments, where the degradation is 14.5% with the "impulsive" scenario and reaches 52% in the "very impulsive" scenario.

The effect of the higher selectivity and attenuation of the "poor" channel is evident when looking at the maximum achieved throughput, which is reduced to nearly 45 Mbit/s. Comparing the "good" and "poor" scenarios in the intersecting SNRs range, we observe that at the same average received SNR, the best performance is obtained with the "poor" channel. For example, at an SNR $= -4$ dB the throughputs of the "impulsive" scenarios, $\mathcal{S}_3$ and $\mathcal{S}_7$, are 5.4 Mbit/s and 15.2 Mbit/s for the "good" and "poor" channels, respectively. In fact, although the SNR value is the same, the working conditions of the two scenarios are very different. In particular, the "good" scenarios have a lower channel attenuation: hence, to achieve the same SNR[7], an higher mean power of the impulsive noise, σ_i^2, is present. In contrast, the "poor" models present a higher signal attenuation and a lower impulsive noise component. Since the impulsive noise is the most detrimental noise source, without clipping, a scenario subjected to a lower σ_i^2 performs better than a scenario with a higher one.

In Fig. 6 and Fig. 7, results with the insertion of the clipping block are illustrated. In particular, results for the "good" scenarios are depicted in Fig. 6. We observe that for the "very impulsive" scenario $\mathcal{S}_4$ the clipping block almost eliminates the effect of the impulsive noise, allowing the system to reach a throughput greater than approximately 86 Mbit/s at all the SNRs. For the scenarios $\mathcal{S}_2$ and $\mathcal{S}_3$ the effects of the clipping block are still relevant and the increase on performance is more evident as the SNRs decrease. In the "impulsive" $\mathcal{S}_3$ scenario the gain on throughput, compared to the case without the clipping block, is present for SNRs less than 14 dB. For example, we observe a gain of approximately 29 Mbit/s and 58 Mbit/s at an SNR $= 5$ dB and -5 dB, respectively. In the "low impulsive" scenario $\mathcal{S}_2$ the improvements of clipping are evident only at SNRs lower than 5 dB, with a gain of nearly 9.6 Mbit/s at an SNR of -5 dB. Finally, in the "quasi-Gaussian" case $\mathcal{S}_1$ the effects of the clipping are negligible and the throughput is the same as in the case without the clipping block for all the SNRs.

An analogous behavior is observed in the "poor" scenarios, as shown in Fig. 7. The best results are obtained with the "very impulsive" scenario $\mathcal{S}_8$, where the mitigation of the effect of the impulsive noise enables the system to reach a throughput greater than 41 Mbit/s for all the SNRs. The insertion of the clipping block provides a significant gain in throughput in the "impulsive" scenario $\mathcal{S}_7$, where the system reaches 31 Mbit/s at an SNR $= -8$ dB. Results for the scenarios $\mathcal{S}_6$ and $\mathcal{S}_5$ show that as the degree of the impulsiveness decreases, the advantages of clipping are less evident, although in the "low impulsive" $\mathcal{S}_6$ scenario a still consistent improvement can be observed for SNRs lower than -5 dB. In the "quasi-Gaussian" case $\mathcal{S}_5$ the performance is the same as without clipping.

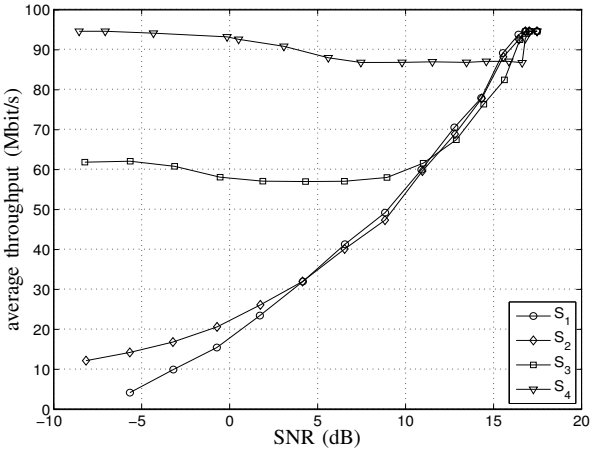

Figure 6. Average HPAV throughput versus average received SNR in "good" scenarios with noise "quasi-Gaussian" (S_1), "low impulsive" (S_2), "impulsive" (S_3) and "very impulsive" (S_4). The clipping block is inserted.

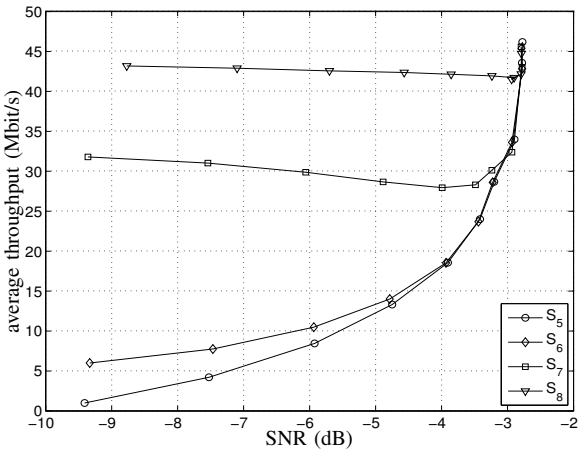

Figure 7. Average HPAV throughput versus average received SNR in "poor" scenarios with noise "quasi-Gaussian" (S_5), "low impulsive" (S_6), "impulsive" (S_7) and "very impulsive" (S_8). The clipping block is inserted.

VII. Conclusions

In this paper, the DLC bit-loading algorithm is presented in the framework of the HPAV technology. To better exploit the error correction capabilities of the turbo

[7]Referring to Section IV we highlight that the PSD of the colored background noise is the same for every channel model.

code this algorithm attempts to maximize the throughput over a set of sub-carriers using a new metric based on the LLRs. It is shown that the DLC outperforms the classical BTC solution in terms of throughput. What is more, the performance of the HPAV system with the DLC algorithm is studied over the channel models proposed by OPERA. In order to simulate the high variability of the power-line channel, eight different scenarios are considered with the introduction of impulsive noise realized by the Middleton's Class A model. Simulation results show that, as the impulsiveness of the channel increases, the performance of the system considerably deteriorates. Furthermore, it is proven that clipping can be a very efficient countermeasure against the impulsive noise, and, as a consequence, even in the more impulsive environments, very promising throughputs can be attained. A possible development of this work could be to adapt the clipping technique when the automatic gain control block is introduced into the system.

APPENDIX

In this section, the computation of the target LLR, $\overline{\ell}^{(T)}$, is described. Two different methods are presented: the first is based on a fixed target approach, while in the second a variable target is employed. In addition, in the variable target case a simplification of the DLC algorithm is given.

A. Fixed target

In Section III-B, considering a single carrier system, the target LLR, $\overline{\ell}^{(m,T)}$, associated to a given target BER for each constellation, is introduced. This suggests a first approximate solution for the multi-modulation case, i.e.

$$\overline{\ell}^{(T)} = \max_{m \in \mathcal{C}} \overline{\ell}^{(m,T)} \tag{18}$$

This target will be denoted as $\overline{\ell}^{(T_1)}$. The solution that employs the constraint (18) is conservative since $\overline{\ell}^{(T_1)}$ appears to be over-dimensioned compared to $\overline{\ell}^{(m,T)}$ for most $m \in \mathcal{C}$. A refinement of this idea is the following: let $\{m_k^{\text{BTC}}\}$ be the bit-loading distribution provided by the BTC algorithm on the set of sub-carrier indices $\mathcal{T}$ and let $\{m_k'^{\text{BTC}}\}$ the immediately higher bit-allocation. The new definition of the target LLR is

$$\overline{\ell}^{(T)} = \max_{k \in \mathcal{T}} \left\{ \max \left\{ \overline{\ell}^{(m_k^{\text{BTC}},T)}, \overline{\ell}^{(m_k'^{\text{BTC}},T)} \right\} \right\}. \tag{19}$$

We observe that $\overline{\ell}^{(m_k^{\text{BTC}},T)}$ is not an increasing monotonic function of m_k^{BTC}, hence the inner maximum of (19) has to be computed. This target will be denoted as $\overline{\ell}^{(T_2)}$.

B. Variable target

In order to obtain a less conservative algorithm, the following target is proposed:

$$\overline{\ell}^{(T)} = \sum_{k \in \mathcal{T}} m_k \cdot \overline{\ell}^{(m_k,T)} \Bigg/ \sum_{k \in \mathcal{T}} m_k \ . \tag{20}$$

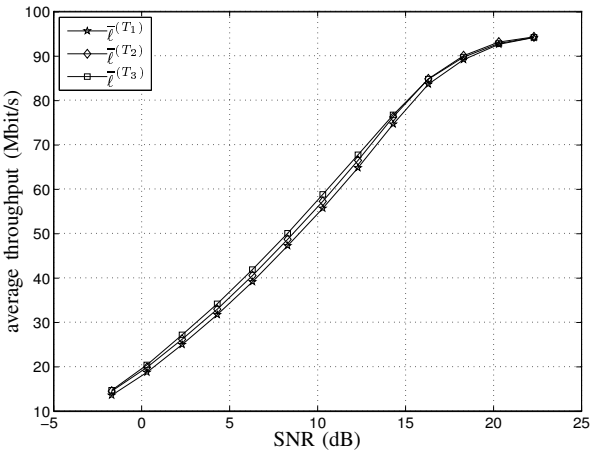

Figure 8. Performance of the DLC algorithm: average HPAV throughput versus average received SNR in a multi-path channel with AWGN noise. Three different target LLRs are adopted: $\overline{\ell}^{(T_1)}$, $\overline{\ell}^{(T_2)}$ and $\overline{\ell}^{(T_3)}$.

This target will be denoted as $\overline{\ell}^{(T_3)}$. It depends on the loaded constellations $\{m_k\}$ with $k \in \mathcal{T}$; therefore, (20) needs to be computed at each iteration of the dichotomic algorithm (point 5 of Section III-B.4) within step c).

Substituting (7) and (20) in (8), the constraint of (12) can be expressed by

$$\overline{\gamma}_{\text{dB}} \geq \overline{\gamma}_{\text{dB}}^{(T)} \tag{21}$$

where $\overline{\gamma}_{\text{dB}} = \sum_{k \in \mathcal{T}} m_k \gamma_{k,\text{dB}}$ and $\overline{\gamma}_{\text{dB}}^{(T)} = \sum_{k \in \mathcal{T}} m_k \gamma_{\text{dB}}^{(m_k,T)}$. Therefore the problem (12) is equivalent to

$$\begin{cases} \max\limits_{\{m_k\} \in \mathcal{C}^{|\mathcal{T}|}} \sum\limits_{k \in \mathcal{T}} m_k \\ \text{s.t. } \overline{\gamma}_{\text{dB}} \geq \overline{\gamma}_{\text{dB}}^{(T)} \end{cases}. \tag{22}$$

The solution of (22) follows the same steps described in III-B.4. More precisely, the metric updating (9) is realized by

$$\overline{\gamma}'_{\text{dB}} = \overline{\gamma}_{\text{dB}} + \sum_{k \in \mathcal{M}} (m'_k - m_k) \gamma_{k,\text{dB}} \tag{23}$$

and the cost (10) is defined by

$$w_k = m'_k (\gamma_{k,\text{dB}} - \gamma_{\text{dB}}^{(m'_k,T)}) - m_k (\gamma_{k,\text{dB}} - \gamma_{\text{dB}}^{(m_k,T)}) \tag{24}$$

With these simplifications it is possible to deal with the received SNRs directly even if the LLR nature of the algorithm is still evident.

In Fig. 8, the performance of the DLC algorithm with the three targets LLR is shown. The best behavior is obtained with the $\overline{\ell}^{(T_3)}$ choice; for example, a gain of nearly 0.28 Mbit/s at 15 dB is observed, in comparison to the $\overline{\ell}^{(T_2)}$ case. Moreover, with this last target, the DLC offers a higher throughput than the DLC with $\overline{\ell}^{(T_1)}$. For example, at 15 dB a gain of nearly 1.5 Mbit/s is observed.

ACKNOWLEDGMENT

The authors wish to express their gratitude to Pietro Menniti, Maria Rosa Borghi and Roberto Gariboldi for continuing support during this work.

REFERENCES

[1] "HomePlug AV baseline specification," May 2007, version 1.1, HomePlug PowerLine Alliance.

[2] "HomePlug AV white paper," http://www.homeplug.org.

[3] L. Guerrieri, P. Bisaglia, G. Dell'Amico, and E. Guerrini, "Performance of the turbo coded HomePlug AV system over power-line channels," in *IEEE ISPLC*, March 2007, pp. 138–143.

[4] L. Guerrieri, E. Guerrini, D. Veronesi, P. Bisaglia, and G. Dell'Amico, "LLR-based bit-loading algorithm for the turbo coded HomePlug AV," in *IEEE GLOBECOM*, Nov. 2007, pp. 140–145.

[5] E. Guerrini, L. Guerrieri, and D. Veronesi, "HomePlug AV system and DLC bit-loading algorithm over OPERA power-line channels with impulsive noise," in *IEEE ISPLC*, April 2008, pp. 164–169.

[6] T. Banwell and S. Galli, "A novel approach to the modeling of the indoor power line channel-Part I: circuit analysis and companion model," in *IEEE Trans. on Power Delivery*, vol. 20, Apr. 2005, pp. 655–663.

[7] S. Galli and T. Banwell, "A novel approach to the modeling of the indoor power line channel-Part II: transfer function and its properties," in *IEEE Trans. on Power Delivery*, vol. 20, July 2005, pp. 1869–1878.

[8] H. Phillips, "Modelling of powerline communication channels," in *IEEE ISPLC*, March 1999, pp. 14–21.

[9] M. Zimmermann and K. Dostert, "A multipath model for the powerline channel," *IEEE Trans. on Commun.*, vol. 50, pp. 553–559, Apr. 2002.

[10] M. Babic, M. Hagenau, K. Dostert, and J. Bausch, "Theoretical postulation of PLC channel model," OPERA, Tech. Rep., March 2005.

[11] "OPERA project," http://www.ist-opera.org.

[12] M. Babic, J. Bausch, T. Kistner, and K. Dostert, "Performance analysis of coded OFDM systems at statistically representative PLC channels," in *IEEE ISPLC*, March 2006, pp. 104–109.

[13] M. Zimmermann and K. Dostert, "Analysis and modeling of impulsive noise in broad-band powerline communications," *IEEE Trans. Electromagn. Compat.*, vol. 44, pp. 249–258, Feb. 2002.

[14] H. A. Suraweera, C. Chai, J. Shentu, and J. Armstrong, "Analysis of impulse noise mitigation techniques for digital television systems," in *Proc. of 8th international OFDM Workshop*, Sept. 2003, pp. 172–176.

[15] L. R. Bahl, J. Cocke, F. Jelinek, and J. Raviv, "Optimal decoding of linear codes for minimizing symbol error rate," *IEEE Trans. on Inform. Theory*, vol. 20, pp. 284–287, March 1974.

[16] J. Vogt and A. Finger, "Improving the max-log MAP turbo decoder," *IEEE Elect. Lett.*, vol. 36, pp. 1937–1939, Nov. 2000.

[17] Wismer and R. Chattergy, *Introduction to nonlinear optimization. System science and engineering*, North-Holland, Ed. Elsevier Science, 1978.

[18] D. Middleton, "Statistical-physical models of electromagnetic interference," *IEEE Trans. Electromagn. Compat.*, vol. 19, pp. 106–127, Aug. 1977.

[19] D. Umehara, H. Yamaguchi, and Y. Morihiro, "Turbo decoding in impulsive noise environment," in *IEEE GLOBECOM*, Nov. 2004, pp. 194–198.

[20] K. H. Kim and S. C. Kim, "Performance analysis of LDPC coded DMT systems with bit-loading algorithms for powerline channel," in *IEEE ISPLC*, March 2007, pp. 234–239.

[21] A. D. Spaulding and D. Middleton, "Optimum reception in an impulsive interference environment-part I: coherent detection," *IEEE Trans. on Comm.*, vol. 25, pp. 910–923, Sep. 1977.

Eleonora Guerrini was born in Lucca, Italy, in 1978. She received her master degree in Telecommunication Engineering from the University of Pisa, Italy, in 2003. In 2004 she spent six months in Austin, Texas, U.S.A., where she worked for StarCore LLC Company developing channel code algorithms for DSP. In 2005 she joined Dora S.p.A., a company of STMicroelectronics Group in Aosta, Italy, where she is currently working on power-line communications.

Lorenzo Guerrieri was born in Aosta, Italy, in 1977. He received his master degree in Mathematics from the University of Bologna, Italy, in 2002. In the same year, he joined DORA S.p.A., today a company of STMicroelectronics Group, in Aosta, Italy. Here he has developed driving algorithms for nematic and bistable liquid crystal display. Since the end of 2004, he has been working on power-line communications.

Daniele Veronesi was born in Rovereto, Italy, on August 04, 1979. He received his master degree in Telecommunication Engineering (2003) from the University of Padova, Padua, Italy. From January 2004 to December 2007, he was a Ph.D. student at the University of Padova. During the academic year 2004-2005, he studied six months at the University of Massachusetts, Amherst (USA) as an exchange student. Since January 2008 he has been collaborating with STMicroelectronics in the design of modems for power-line. His major interests are in power control for cellular systems, cooperative communication and power-line communication.

Paola Bisaglia was born in Padova, Italy, on August 8, 1971. She received her master and Ph.D. degrees in Electronic Engineering from the University of Padova, Padua, Italy in 1996 and 2000 respectively. In 2000 she joined Hewlett-Packard Research Laboratories in Bristol, England, where she worked on home phone-line networking and wireless LANs. From 2002 to 2005 she was a research fellow at the Department of Information Engineering of the University of Padova, Italy, investigating pre- and post-detection strategies for next generation (4G) broadband cellular systems. She has been with Dora S.p.A., a company of STMicroelectronics Group, since May 2005, where she is involved in research activities and in the design of integrated circuits for narrow-band and wide-band power-line communications dedicated to indoor and outdoor applications.

Roberto Cappelletti was born in Milan, Italy, in September 1966. He received his master degree in Electronic Engineering from the Politecnico di Milano, Milan, Italy in 1995. In the same year he joined Siemens Telecommunications R&D Group in Milan, Italy, where he worked on the design of base band equipments for radio-bridges. In 1996 he joined STMicroelectronics, Milan, Italy, where he has been involved, since 1998, in research activities and design of power-line modems. Today he is leading a design team dedicated to the design of integrated circuits for power-line communication, motion control, high voltage gate driver and industrial ASIC.